Supporting Information

Tuning the electron transfer events in a series of cyanide-bridged $[Fe_2Co_2]$ squares according to different electron donors

Lingyi Meng,[a] Yi-Fei Deng,*[a] Jianxun Liu,[b] Yan Jun Liu[b] and Yuan-Zhu Zhang*[a]

[a]Department of Chemistry, Southern University of Science and Technology (SUSTech), Shenzhen 518055, China

[b]Department of Electrical and Electronic Engineering, Southern University of Science and Technology (SUSTech), Shenzhen, 518055, China

Email: dengyf@sustech.edu.cn; zhangyz@sustech.edu.cn

Experimental section

Materials and physical measurements. $[NBu_4][Tp^*Fe(CN)_3]$ and 4-hydroxymethyl-4'-methyl-2,2'-bipyridine (L2) were synthesized according to the previous literatures.[1,2] All other chemicals and reagents were commercially available and used without further purification. FT-IR spectra were recorded in the range 600 - 4000 cm^{-1} on a Bruker tensor II spectrophotometer. Variable temperature data was obtained by using liquid nitrogen cooled and evacuated Specac Golden Gate low temperature ATR accessories. The TGA measurements were carried out on freshly filtered crystals using the METTLER TOLEDO TGA2 instrument in an insert argon atmosphere over a temperature range of 30 - 500 °C with a heating rate of 3 °C / min. Elemental analyses (C, H, N) were measured by a vario EL cube CHNOS Elemental Analyzer Elementar Analysensysteme GmbH. The PXRD measurements were recorded at room temperature on a Rigaku Smartlab X-ray diffractometer with Cu Kα radiation (45 kV, 200 mA) between 5 and 50° (2θ). The simulated patterns are calculated from the single crystal data. Variable-temperature UV-Vis spectra were obtained on a Craic Technologies microspectrophotometer. Magnetic susceptibility data under 1 kOe dc field were collected at temperatures between 2 - 400 K using a SQUID MPMS3 magnetometer. For the photomagnetic experiments, irradiation was performed on the fresh sample at 10 K, light from an infrared diode laser (20 mW, 808 nm; MDL-III-808 nm-19060627, Changchun New Industries Optoelectronics Technology Co., Ltd (CNI)) was guided via a flexible optical fiber (5 m length; CNI Fiber) into the SQUID magnetometer. Sample temperatures were corrected for light-induced heating effect (avg. +4 K for the red light), which was referenced to the data collected in the absence of light. Magnetic data were corrected for the diamagnetism of the sample holder and for the diamagnetism of the sample using Pascal's constants.[2]

X-ray crystallographic data. The single crystal data for complexes **1 - 3** were collected on a Bruker D8 VENTURE diffractometer with graphite monochromated Mo Kα radiation (λ = 0.71073 Å). Lorentz/polarization corrections were applied during data reduction and the structures were solved by the direct method (SHELXS-2014).[3] Refinements were performed by full-matrix least squares (SHELXL-2014) on F^2 and empirical absorption corrections (SADABS) were applied.[4] Anisotropic thermal parameters were used for the non-hydrogen atoms. Hydrogen atoms were added geometrically and refined using a riding model. Weighted R factors (wR) and all the goodness-of-fit (S) values are based on F2; conventional R factors (R) are based on F, with F set to zero for negative F^2. CCDC-2036955 (**1**-100 K), 2125435 (**2**-280 K), 2125434 (**2**-100 K), 2125436 (**3**-110 K), contains the crystallographic data that can be obtained via www.ccdc.cam.ac.uk/conts/retrieving.html (or from the Cambridge Crystallographic Data Centre, 12, Union Road, Cambridge CB21EZ, UK; fax: (+44) 1223-336-033; or deposit@ccdc.cam.ac.uk).

Caution: Although no such issues happened during the present work, perchlorate salts are potentially explosive and should be handled in small quantities and with great care.

Synthesis of $\{[(Tp^*)Fe(CN)_3Co(L1)_2]_2[ClO_4]_2\}\cdot 4MeCN\cdot 2H_2O$ (**1**)

4-formyl-4'-methyl-2,2'-bipyridine (19.8 mg, 0.1 mmol) was treated with $Co(ClO_4)_2·6H_2O$ (18.3 mg, 0.05 mmol) in acetonitrile (5 mL) to afford a yellow solution that was allowed to stir for 30 min. $[NBu_4][(Tp^*)Fe(CN)_3]$ (33.6 mg, 0.05 mmol) was subsequently added and the mixture was stirred for 3 h and filtered. The red filtrate was layered with Et_2O to afford dark red block crystals of **1** (yield: 23.9 mg, 22%). FT-IR (cm^{-1}; 293 K): ν = 2534 (m, ν_{BH}), 2152 (s, ν_{CN}), 2123 (w, ν_{CN}). Anal. Calcd $C_{92}H_{100}B_2Cl_2Co_2Fe_2N_{30}O_{14}$: C, 50.87; H, 4.64; N, 19.35. Found: C, 50.58; H, 4.71; N, 19.22.

Synthesis of $\{[(Tp^*)Fe(CN)_3Co(L2)_2]_2[ClO_4]_2\}·3MeCN$ (**2**)

Complex **2** was obtained in a similar way to complex **1**, by using 4-hydroxymethyl-4'-methyl-2,2'-bipyridine (20.0 mg, 0.1 mmol) instead (yield: 16.5 mg, 16%). FT-IR (cm^{-1}; 293 K): ν = 2529 (m, ν_{BH}), 2155 (s, ν_{CN}), 2120 (w, ν_{CN}). Anal. Calcd $C_{90}H_{99}B_2Cl_2Co_2Fe_2N_{29}O_{12}$: C, 51.40; H, 4.71; N, 19.32. Found: C, 51.31; H, 4.85; N, 19.27.

Synthesis of $\{[(Tp^*)Fe(CN)_3Co(L3)_2]_2[ClO_4]_2\}·4MeOH$ (**3**)

[2,2'-bipyridine]-4,4'-dimethanol (10.8 mg, 0.05 mmol) was treated with $Co(ClO_4)_2·6H_2O$ (9.2 mg, 0.025 mmol) in a mixture of acetonitrile and methanol (1:1, V/V, 4 mL) to afford a yellow solution that was allowed to stir for 30 min. The methanol solution (2 mL) of $[NBu_4][(Tp^*)Fe(CN)_3]$ (16.8 mg, 0.025 mmol) was subsequently added and the mixture was stirred for 3 h and filtered. The red filtrate was layered with Et_2O to afford dark red block crystals of **3** (yield: 56.5 mg, 52%). FT-IR (cm^{-1}; 303 K): ν = 2535 (m, ν_{BH}), 2153 (s, ν_{CN}). Anal. Calcd $C_{88}H_{108}B_2Cl_2Co_2Fe_2N_{26}O_{20}$: C, 48.62; H, 4.97; N, 16.76. Found: C, 48.47; H, 5.06; N, 16.67.

Table S1. The crystallographic data and structural parameters for **1** – **3**.

Complex	**1**	**2**		**3**
Temperature / K	100(2)	100(2)	280(2)	110(2)
CCDC	2036955	2125434	2125435	2125436
Formula	$C_{92}H_{100}B_2Cl_2Co_2Fe_2N_{30}O_{14}$		$C_{90}H_{99}B_2Cl_2Co_2Fe_2N_{29}O_{12}$	$C_{88}H_{108}B_2Cl_2Co_2Fe_2N_{26}O_{20}$
Molecular weight / g mol^{-1}	2171.92		2101.06	2172.05
Crystal system	Monoclinic		Triclinic	Triclinic
Space group	$P2_1/c$		$P\bar{1}$	$P\bar{1}$
Crystal size / mm	0.4×0.3×0.3		0.5×0.4×0.3	0.5×0.4×0.2
Wavelength / Å	0.71073		0.71073	0.71073
Crystal colour	red	green	red	green
a / Å	13.9683(9)	12.017(2)	12.331(6)	11.8997(8)
b / Å	31.1073(17)	14.179(2)	14.352(6)	14.1917(11)
c / Å	22.8137(13)	15.527(3)	15.960(6)	15.8456(12)
α / deg	90	81.971(5)	82.594(13)	85.221(3)
β / deg	99.024(2)	73.964(5)	74.147(14)	74.071(3)
γ / deg	90	79.688(6)	80.292(14)	79.083(2)
V / Å^3	9790.2(10)	2490.2(7)	2668(2)	2525.2(3)
Z	4	1	1	1
D_{cal} / g cm^{-3}	1.378	1.401	1.232	1.418
μ / mm^{-1}	0.750	0.740	0.686	0.736
F (000)	4192.0	1088.0	1024.0	1112.0
Data/restraints/parameters	21663/1743/1221	8507/55/661	9258/41/600	8847/14/659
Reflections collected	89636	17545	20066	20311
2θ range / °	4.49 - 54.356	5.028 - 49.998	4.816 - 50	5.03 - 50.05
Completeness	100%	97.1%	98.6%	99.5%
Residual map / e Å^{-3}	1.64/-1.63	1.86/-0.87	1.25/-0.67	1.88/-1.24
Goodness-of-fit on F^2	1.033	1.038	1.077	1.019
Final indices[I>2σ(I)]	R_1 = 0.0909, wR_2 = 0.2463	R_1 = 0.1053, wR_2 = 0.2474	R_1 = 0.0942, wR_2 = 0.2445	R_1 = 0.0911, wR_2 = 0.2523
R indices (all data)	R_1 = 0.1382, wR_2 = 0.2789	R_1 = 0.1472, wR_2 = 0.2951	R_1 = 0.1367, wR_2 = 0.2984	R_1 = 0.1316, wR_2 = 0.2870

Table S2. Selected bond lengths [Å] and angles [deg] for **1** at 100 K.

	1
Fe1-C1	1.912(6)
Fe1-C2	1.905(6)
Fe1-C3	1.925(6)
Fe1-N4	1.995(5)
Fe1-N6	1.991(5)
Fe1-N8	2.011(5)
Fe-C (average)	1.914
Co1-N1	2.081(5)
Co1-N10	2.124(5)
Co1-N11	2.097(5)
Co1-N12	2.090(5)
Co1-N13	2.142(5)
Co1-N14	2.040(5)
Co-N (average)	2.096
C1-Fe1-N8	90.6(2)
C1-Fe1-N6	177.6(2)
C1-Fe1-N4	89.4(2)
C1-Fe1-C3	90.4(3)
C1-Fe1-C2	87.2(2)
N1-Co1-N14	91.35(19)
N1-Co1-N13	171.4(2)
N1-Co1-N12	95.42(19)
N1-Co1-N11	95.24(19)
N1-Co1-N10	84.18(19)
Fe1-C1-N1	176.5(5)
Fe1-C2-N2	175.5(5)
Co1-N1-C1	162.2(5)
Co2-N2-C2	167.8(4)

Table S3. Selected bond lengths [Å] and angles [deg] for **2** at 100 and 280 K.

	100 K	280 K
Fe1-C1	1.880(7)	1.916(6)
Fe1-C2	1.881(7)	1.905(7)
Fe1-C3	1.921(9)	1.926(9)
Fe1-N4	2.014(6)	1.993(6)
Fe1-N6	2.020(6)	1.999(5)
Fe1-N8	2.041(6)	2.018(5)
Fe-C (average)	1.894	1.916
Co1-N1	1.918(6)	2.081(6)
Co1-N10	1.982(7)	2.139(6)
Co1-N11	1.963(7)	2.105(6)
Co1-N12	1.963(7)	2.107(6)
Co1-N13	1.966(7)	2.122(6)
Co1-N2A	1.904(6)	2.058(6)
Co-N (average)	1.949	2.102
C1-Fe1-N8	89.2(3)	89.6(2)
C1-Fe1-N6	175.1(3)	177.1(3)
C1-Fe1-N4	89.7(3)	90.0(3)
C1-Fe1-C3	91.53)	89.5(3)
C1-Fe1-C2	89.83)	87.7(3)
N1-Co1-N13	95.5(3)	173.2(2)
N1-Co1-N12	176.8(3)	97.3(3)
N1-Co1-N11	89.8(3)	92.6(2)
N1-Co1-N10	86.7(2)	85.4(2)
N1-Co1-N2A	90.6(2)	91.9(2)
Fe1-C1-N1	176.6(6)	174.5(6)
Fe1-C2-N2	172.5(6)	174.5(6)
Co1-N1-C1	162.3(6)	163.1(5)
Co1A-N2-C2	168.0(6)	169.3(5)

Symmetry transformations used to generate equivalent atoms: A 1-x, 1-y, 1-z.

Table S4. Selected bond lengths [Å] and angles [deg] for **3** at 110 K.

	3
Fe1-C1	1.879(7)
Fe1-C2	1.878(8)
Fe1-C3	1.891(7)
Fe1-N4	2.021(6)
Fe1-N6	2.042(6)
Fe1-N8	2.017(6)
Fe-C (average)	1.883
Co1-N1	1.885(6)
Co1-N2A	1.892(6)
Co1-N10	1.929(5)
Co1-N11	1.954(6)
Co1-N12	1.931(6)
Co1-N13	1.939(6)
Co-N (average)	1.922
C1-Fe1-N4	92.8(2)
C1-Fe1-N6	176.6(2)
C1-Fe1-N8	93.7(3)
C1-Fe1-C2	90.9(3)
C1-Fe1-C3	84.9(3)
N1-Co1-N2A	90.5(2)
N1-Co1-N10	94.2(2)
N1-Co1-N11	176.6(2)
N1-Co1-N12	91.2(2)
N1-Co1-N13	89.9(2)
Fe1-C1-N1	173.7(5)
Fe1-C2-N2	175.5(6)
Co1A-N2-C2	164.8(5)
Co1-N1-C1	168.8(5)

Symmetry transformations used to generate equivalent atoms: A 1-x, -y, 1-z.

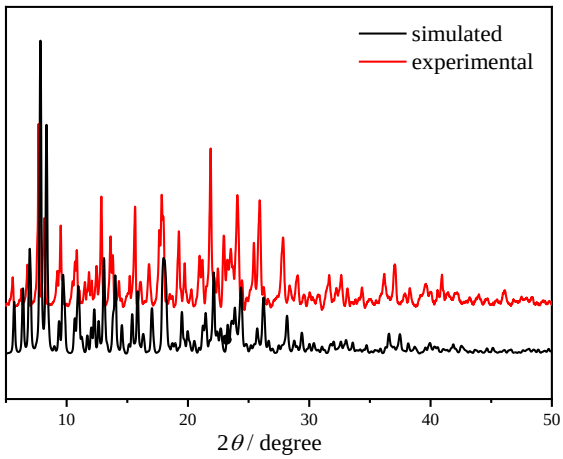

Fig. S1 The powder X-ray diffraction data for **1**. The simulated patterns are calculated from the single crystal data.

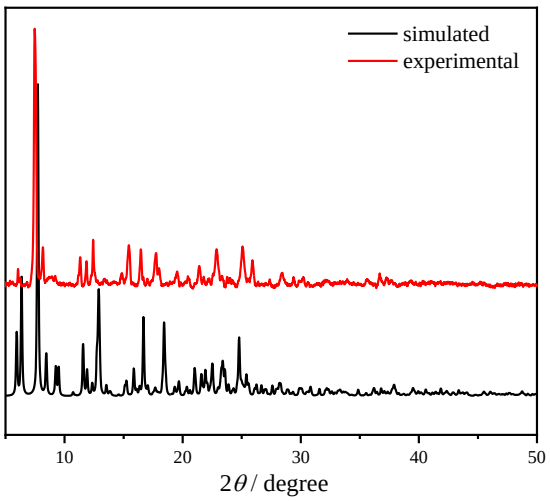

Fig. S2 The powder X-ray diffraction data for **2**. The simulated patterns are calculated from the single crystal data.

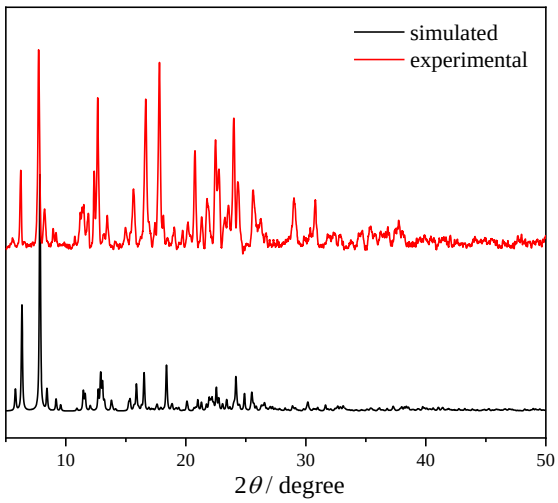

Fig. S3 The powder X-ray diffraction data for **3**. The simulated patterns are calculated from the single crystal data.

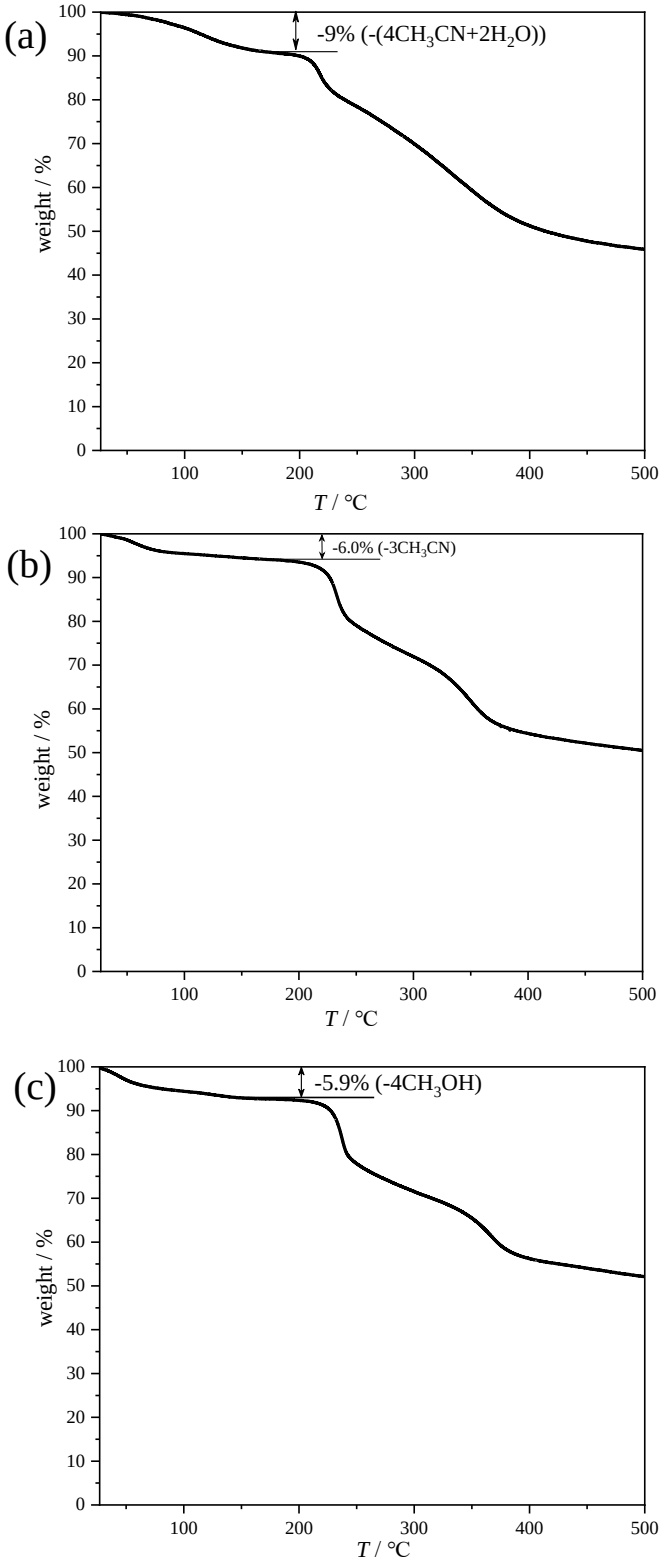

Fig. S4 TGA plots for **1** (a), **2** (b) and **3** (c).

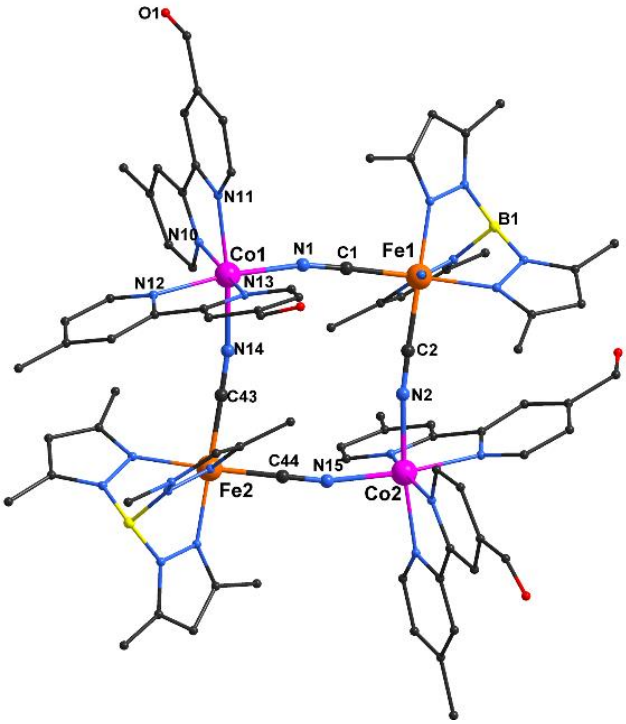

Fig. S5 [Fe_2Co_2] square present in structures of **1** at 100 K. All the counter ions, lattice solvents and hydrogen atoms are omitted for clarity.

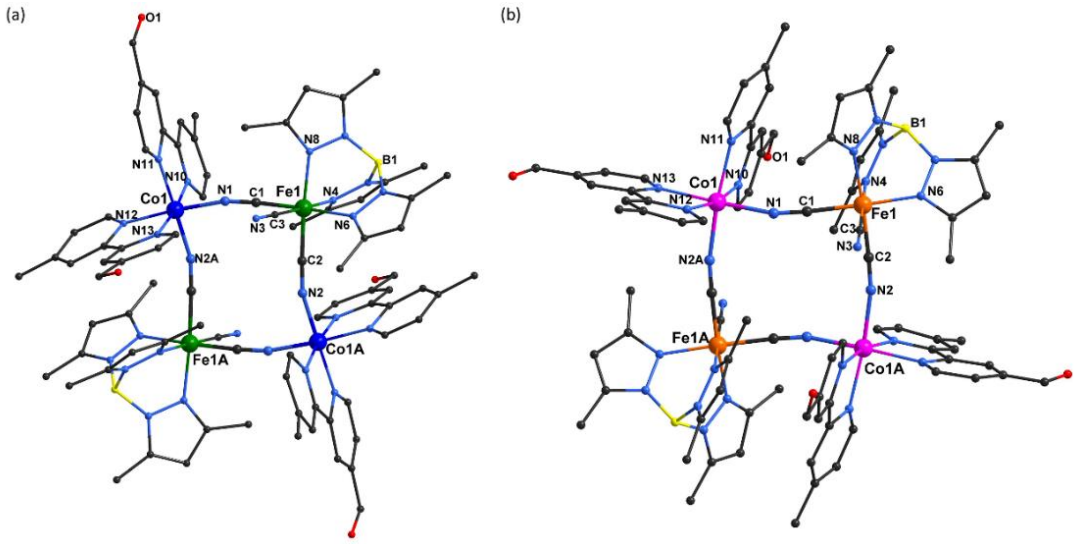

Fig. S6 [Fe_2Co_2] square present in structures of **2** at 100 K (a) and 280 K (b). All the counter ions, lattice solvents and hydrogen atoms are omitted for clarity.

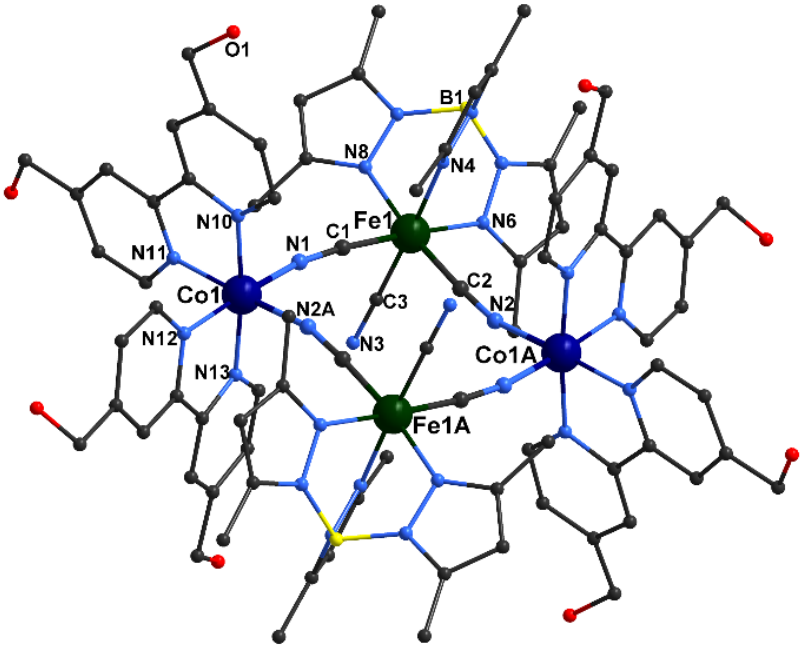

Fig. S7 [Fe_2Co_2] square present in structures of **3** at 110 K. All the counter ions, lattice solvents and hydrogen atoms are omitted for clarity.

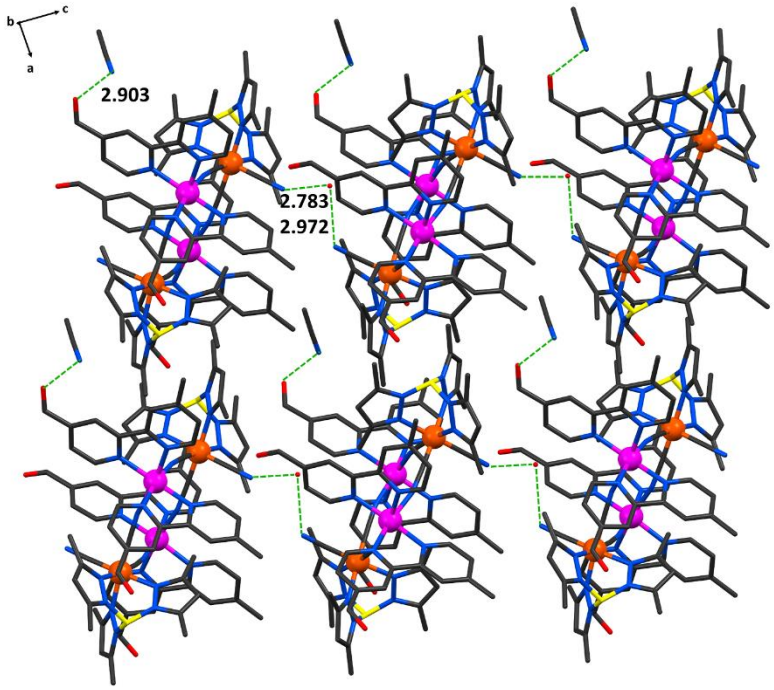

Fig. S8 Packing diagram for **1** at 100 K showing the hydrogen bonding interactions between H_2O and terminal cyanides ($O_{H2O}\cdots N_{CN}$: 2.783, 2.972 Å), and between MeCN and L1 ligands ($N_{MeCN}\cdots O_{L1}$: 2.903 Å). Hydrogen atoms and counter anions are omitted for clarity.

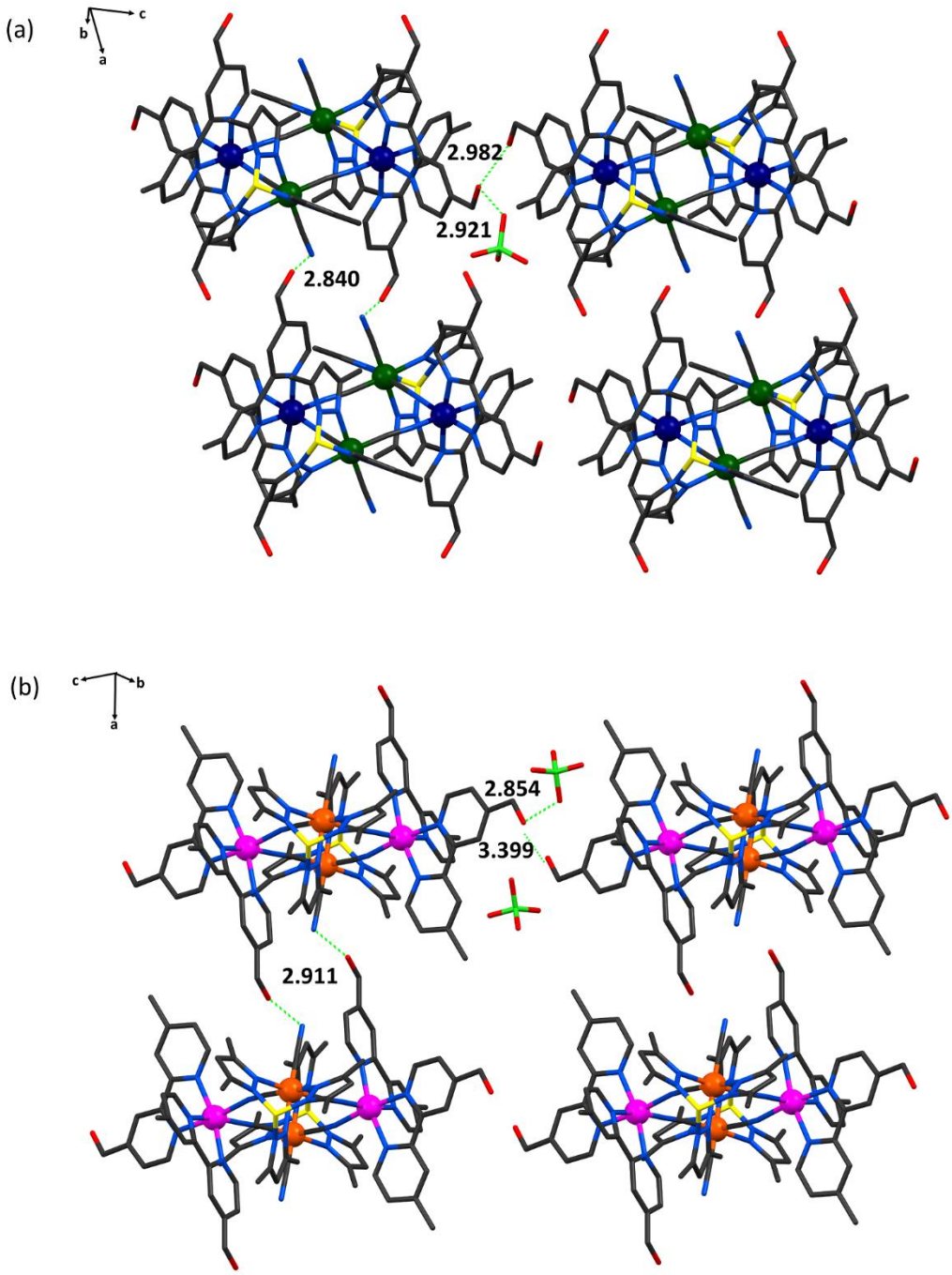

Fig. S9 Packing diagrams for **2** at 100 K (a) and 280 K (b) showing the hydrogen-bonding interactions between the neighboring L2 ligands ($O_{L2}\cdots O_{L2}$: 2.982 Å (100 K), 3.399 Å (280 K)), L2 and $[ClO_4]^-$ ($O_{L2}\cdots O_{ClO4}$: 2.921 Å (100 K), 2.854 Å (280 K)), and between L2 and terminal cyanides ($O_{L2}\cdots N_{CN}$: 2.840 Å (100 K), 2.911 Å (280 K)). Hydrogen atoms, counter anions and solvent molecules are omitted for clarity.

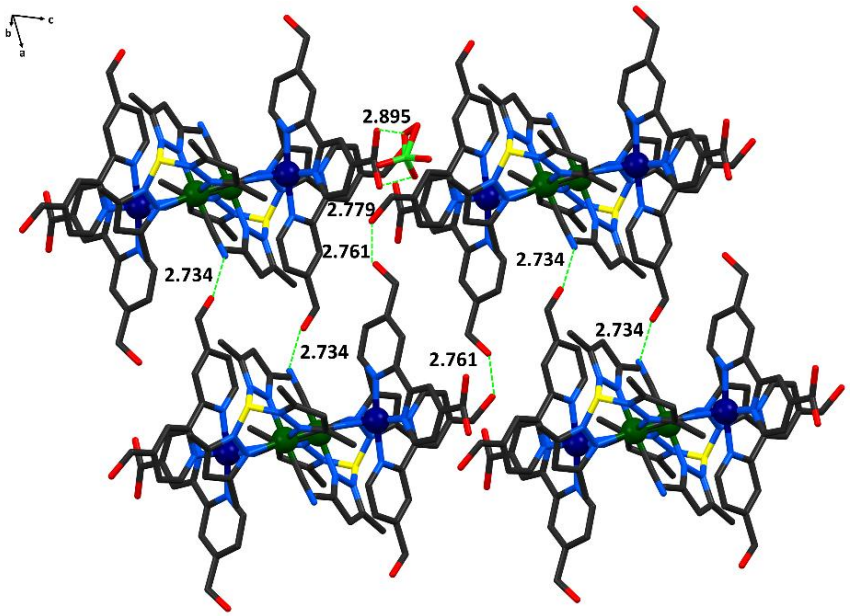

Fig. S10 Packing diagram for **3** at 110 K showing the hydrogen-bonding interactions between the adjacent L3 ligands ($O_{L3}\cdots O_{L3}$: 2.761 Å), L3 and $[ClO_4]^-$ ($O_{L3}\cdots O_{ClO4}$: 2.779, 2.895 Å), and between L3 and terminal cyanides ($O_{L3}\cdots N_{CN}$: 2.734 Å). Hydrogen atoms, counter anions and solvent molecules are omitted for clarity.

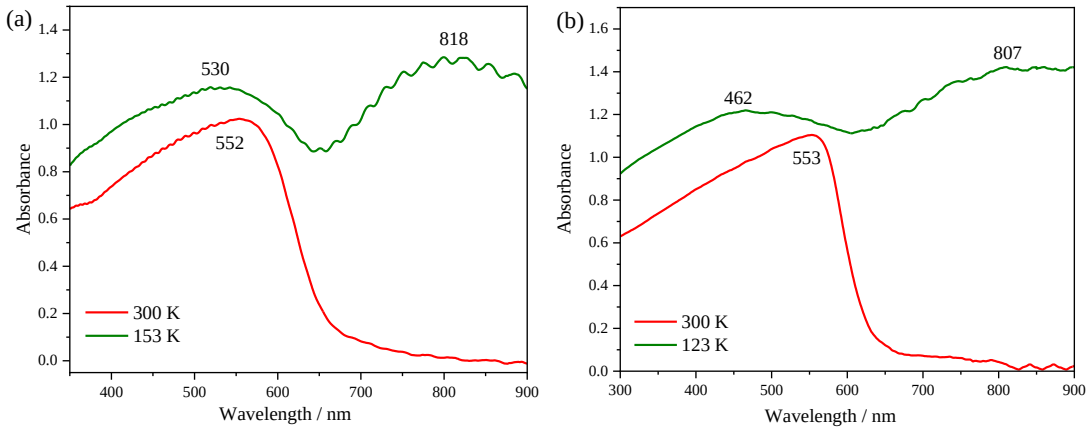

Fig. S11 Variable-temperature solid-state UV-Vis spectra for **2** (a) and **3** (b).

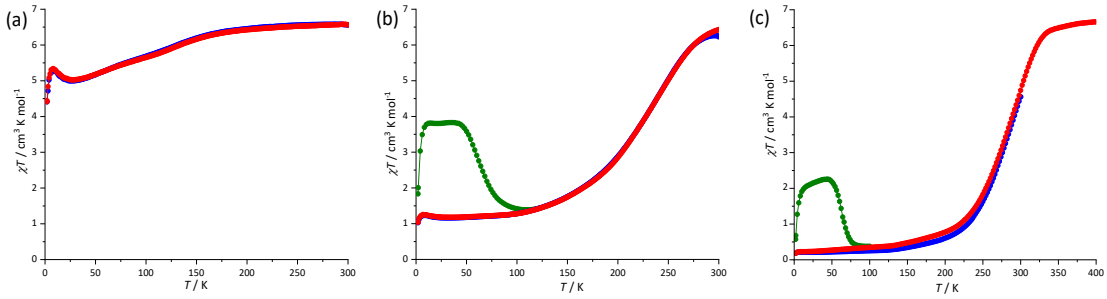

Fig. S12 Variable temperature magnetic susceptibility data for **1** (a), **2** (b) and **3** (c) collected in the dark (1 kOe; blue, cooling; red, heating) and after light irradiation (green, 808 nm, 20 mW, 10 kOe). Solid lines are guides for the eye.

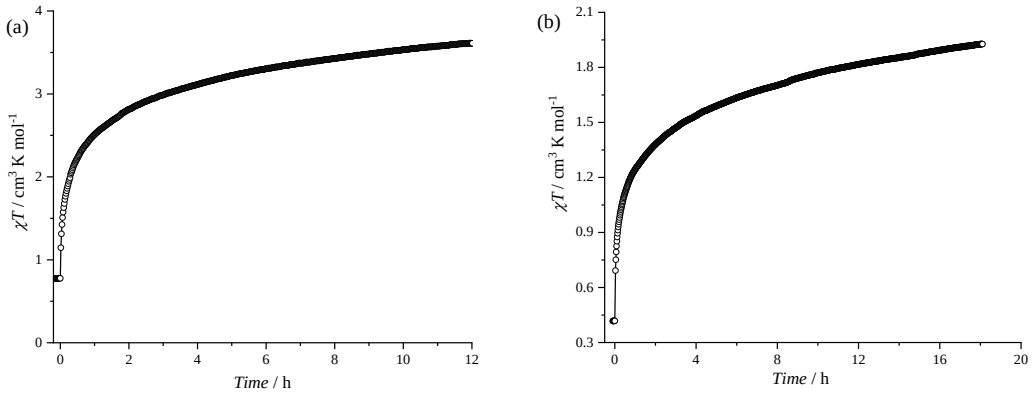

Fig. S13 Time evolution of the χT products of **2** (a) and **3** (b) under light irradiation (808 nm, 20 mW) at 10 K and 10 kOe dc field. Solid lines are guides for the eye.

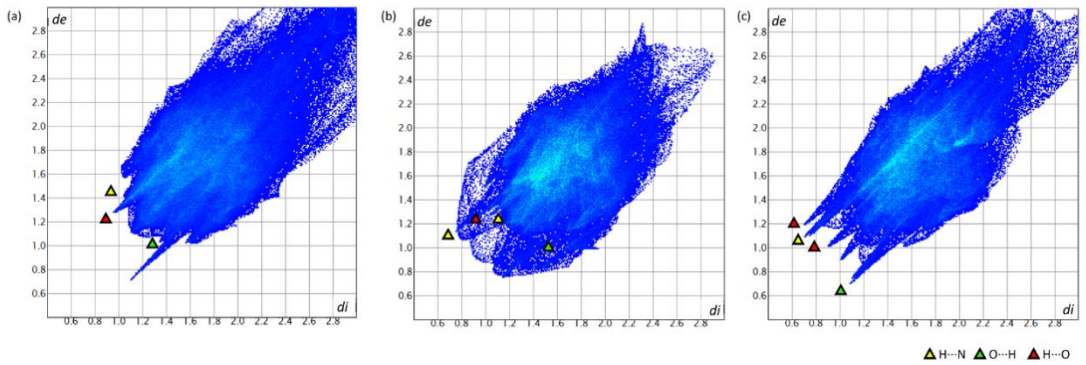

Fig. S14 Hirshfeld surfaces associated with the fingerprint plots for the cationic square cores $[Fe_2Co_2]^{2+}$ of **1** (a), **2** (b) and **3** (c). The spikes labelled with yellow (H···N), light green (O···H) and red (H···O) triangles depict the characteristic features of the fingerprint plots.

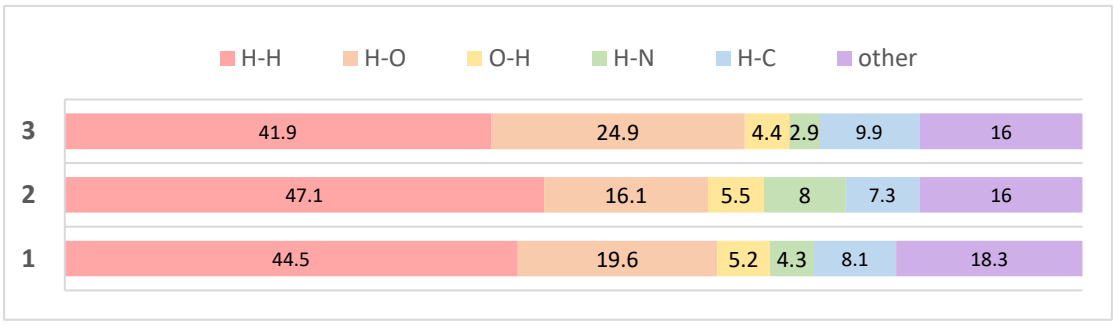

Fig. S15 Percentage contributions of the various close intermolecular contacts to the Hirshfeld surface area in **1** - **3**.

References

1 L. Meng, Y. F. Deng, S. Liu, Z. Zheng and Y. Z. Zhang, *Sci. China: Chem.*, 2021, **64**, 1340−1348;

2 L. Della Ciana, I. Hamachi and T. J. Meyer, *J. Org. Chem*., 1989, **54**, 1731−1735.

3 G. A. Bain and J. F. Berry, *J. Chem. Educ.*, 2008, **85**, 532-536.

4 (a) G. M. Sheldrick, *SHELXL-2014*, Program for the solution of crystal structures. University of Göttingen, Göttingen, Germany, **2014**; (b) G. M. Sheldrick, *SHELXL-2014*, Program for crystal structure refinement. University of Göttingen, Göttingen, Germany, **2014**; (c) G. M. Sheldrick. *SADABS*, v.2.01, Bruker/Siemens area detector absorption correction program. Bruker AXS, Madison, Wisconism, **1998**.